# Analysis of a vibro-impact nonlinear energy sink: theoritical and numerical developments

Tao Li, Sébastien Seguy, Alain Berlioz, Etienne Gourc

# Analysis of a Vibro-Impact Nonlinear Energy Sink: Theoretical and Numerical Developments

**T. LI[a] , S. SEGUY[a], A. BERLIOZ[b], E. GOURC[c]**

a. Université de Toulouse; INSA; ICA (Institut Clément Ader), F-31077 Toulouse, France.E-mail : tli, seguy@insa-toulouse.fr
b. Université de Toulouse; UPS; ICA (Institut Clément Ader); F-31062 Toulouse, France. E-mail : alain.berlioz@univ-tlse3.fr
c.Federal University of Uberlândia,FEMEC,LMEst,Uberlândia - MG, 38408-10, Brazil. E-mail :etienne.gourc@gmail.com

## Abstract :

*Recently, it has been demonstrated that a Vibro-Impact type Nonlinear Energy Sink (VI-NES) can be used efficiently to mitigate vibration of a Linear Oscillator (LO) under transient loading and harmonic force. In this paper, a design optimization procedure of an optimal VI-NES coupled to LO for energy pumping is presented theoretically and numerically. Due to the small mass ratio between the flying mass of the VI-NES and LO, the obtained equation of motion is possible to use the method of multiple scales in the case of 1:1 resonance. It is showed that there exist different response regimes like Strongly Modulated Response (SMR) proved to be the most efficient reponse regime for vibration reduction. An optimization procedure is presented and the results are verified numerically.*

**Key words: Dynamics, Nonlinear Energy Sink, Vibro-Impact,Targeted Energy Transfer**

## 1 Introduction

Targeted Energy Transfer (TET) has been widely studied during the last decade. In this context, a small mass, Nonlinear Energy Sink( NES), is used to mitigate any unwanted disturbance introduced in a primary system (i.e. LO) by efficiently transferring and eliminating energy from the main system to the NES.

Energy pumping under transient loading has been extensively studied. In [1, 2] it has been shown that the main phenomena allowing TET is based on the 1 : 1 resonance capture. Experimental verifications are presented in [3, 4, 5].

TET under external forcing has also been studied. Introduction of a suitable asymptotic procedure based on the invariant manifold approach [6] has shown that in addition to periodic regimes, system with NES can exhibit beating response, referred as strongly modulated response [7]. This type of response has been verified experimentally in [8]. The use of NES to passively control instability is also a growing interest. In [9], a NES is used to control limit cycle oscillation of a Van der Pol system. The effectiveness of a NES to suppress aeroelastic instability is studied in [10, 11, 12, 13]. In [14] , it is shown that a NES can be used to control chatter instability in turning.

All the aforementioned studies deal with NES with cubic non-linearity. Recent studies have enlightened that non-smooth system can be used as NES. One of the main advantages of this type of NES over classic NES is that they are often easier to build. Gendelman investigated energy transfer in system with non-polynomial nonlinearity [15]. NES with piecewise linear stiffness have been studied in [16] under transient and periodic forcing. The case of a vertical NES, considering its own weight has been reported in [17]. Vibro-impact type NES (VI-NES) have been studied in [18, 19, 20]. However, these studies were concentrated around numerical simulations. In [21], the invariant manifold approach has been extended to VI-NES under transient loading. In a recent study, the potential of a VI-NES to mitigate vibrations of a LO subjected to a harmonic excitation is investigated theoretically and experimentally in [22], however the optimization of the TET and presentation of an optimal VI-NES are left to be done.

The objective of the paper is to present a design procedure of an optimal VI-NES. The structure of the paper is organized as follows. The first part is devoted to the theoretical treatment of the equation of motion. In the second part, four typical response regimes are observed by changing parameters and their efficiency of TET is compared. In the next section, a VI-NES optimization procedure is presented. Section 4 incorporates the concluding remarks.

## 2 Mechanical model

The system considered is composed of a linear oscillator (LO) with an embedded Vibro-Impact Nonlinear Energy Sink (VI-NES). The LO is subjected to an imposed base displacement. The system is presented in Fig.1.

The governing equations of motion between impacts are expressed as:

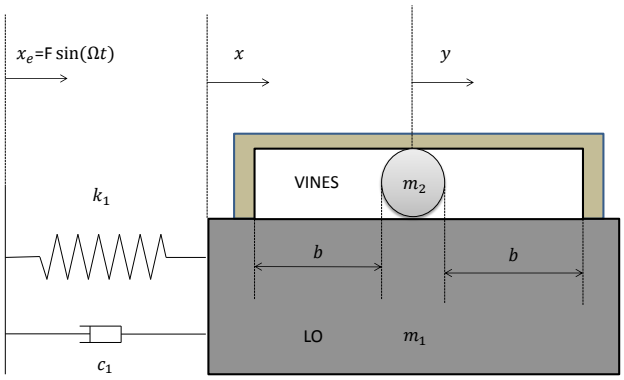


Figure 1: Schema of a LO coupled to VI-NES

$$\begin{aligned} &m_1 \frac{d^2}{dt^2} x(t) + c_1 \frac{d}{dt} x(t) + k_1 x(t) = k_1 x_e(t) + c_1 \frac{d}{dt} x_e(t) \\ &m_2 \frac{d^2}{dt^2} y(t) = 0 \\ &\forall |x - y| < b \end{aligned} \tag{1}$$

Where $x$ and $y$ are the displacement of LO and VI-NES respectively. $x_e$ is the displacement imposed by the exciting base in the following way:

$$x_e(t) = F \sin(\Omega t) \tag{2}$$

When $|x - y| = b$, an impact takes place. The state of the system after impact is obtained using the simplified shock theory and the condition of total momentum conservation:

$$\begin{aligned} &x_+ = x_-, y_+ = y_- \\ &m_1 \dot{x}_+ + m_2 \dot{y}_+ = m_1 \dot{x}_- + m_2 \dot{y}_- \\ &\dot{x}_+ - \dot{y}_+ = R(\dot{x}_- - \dot{y}_-) \\ &for\, |x - y| = b \end{aligned} \tag{3}$$

The dots denote differentiation with respect to $t$, indices + and - denote the instant immediately after and before the impact. $R \in [0, 1]$ is the restitution coefficient of impact. Change of variables is introduced in the following way:

$$\begin{aligned} &\epsilon = \frac{m_2}{m_1}, {\omega_0}^2 = \frac{k_1}{m_1}, \tau = \omega_0 t, \lambda = \frac{c_1}{m_2 \omega_0}, \omega_1 = \frac{\omega}{\omega_0} \\ &\frac{F}{b} = \epsilon G, x = Xb, y = Yb \end{aligned} \tag{4}$$

The reduced governing equation of motion between impact are as follow:

$$\begin{aligned}&\frac{d^2}{d\tau^2}X(\tau)+\varepsilon\lambda\frac{d}{d\tau}X(\tau)+X(\tau)=\epsilon G\sin(\omega_1\tau)+\lambda\epsilon^2G\omega_1\cos(\omega_1\tau)\\&\epsilon\frac{d^2}{d\tau^2}Y(\tau)=0\\&\forall|X-Y|<1\end{aligned}\tag{5}$$

The reduced governing equation of collision are expressed as:

$$\begin{aligned}&X_+=X_-,Y_+=Y_-\\&\dot{X}_+-\dot{Y}_+=R(\dot{X}_--\dot{Y}_-)\\&m_1\dot{X}_++m_2\dot{Y}_+=m_1\dot{X}_-+m_2\dot{Y}_-\\&for\,|X-Y|=1\end{aligned}\tag{6}$$

New variables representing the displacement of the center of mass and the internal displacement of VI-NES are introduced as follow:

$$v(\tau)=X(\tau)+\epsilon Y(\tau),w(\tau)=X(\tau)-Y(\tau)\tag{7}$$

Substituting of (7) into the equation (5) and (6) , equations between impact become:

$$\begin{aligned}&\frac{d^2}{d\tau^2}v(\tau)+\frac{\lambda\epsilon\left(\frac{d}{d\tau}v(\tau)+\epsilon\frac{d}{d\tau}w(\tau)\right)}{1+\epsilon}+\frac{v(\tau)\epsilon+w(\tau)}{1+\epsilon}\\&=\epsilon G\sin(\omega_1\tau)+\lambda\epsilon^2G\omega_1\cos(\omega_1\tau)\\&\frac{d^2}{d\tau^2}w(\tau)+\frac{\lambda\epsilon\left(\frac{d}{d\tau}v(\tau)+\epsilon\frac{d}{d\tau}w(\tau)\right)}{1+\epsilon}+\frac{v(\tau)+\epsilon w(\tau)}{1+\epsilon}\\&=\epsilon G\sin(\omega_1\tau)+\lambda\epsilon^2G\omega_1\cos(\omega_1\tau)\\&\forall|w|<1\end{aligned}\tag{8}$$

and the impact condition equation (6) is rewritten as follows:

$$\begin{aligned}&w_+=w_-,v_+=v_-\\&w_+=Rw_-,v_+=v_-\\&for\,|w|=1\end{aligned}\tag{9}$$

In the context of energy pumping, the mass ratio $\epsilon$ is supposed to be small ($\approx 1\%$). In this case,Eq.(8) may be analyzed by Mutiple Scales Method with respect to this small parameter. The solutions are searched to the second order as follow:

$$\begin{aligned}&v(\tau,\epsilon)=v_0(\tau_0,\tau_1)+\epsilon v_1(\tau_0,\tau_1)\\&w(\tau,\epsilon)=w_0(\tau_0,\tau_1)+\epsilon w_1(\tau_0,\tau_1)\\&\tau_k=\epsilon^0\tau+\epsilon^1\tau\end{aligned}\tag{10}$$

Substituting of (10) into (9) and (8), and after cancel the same power of $\epsilon$, gives:

$$\begin{aligned}
&\epsilon^0 : \\
&\quad \frac{\partial^2}{\partial {T_0}^2} v_0 (T_0, T_1) + v_0 (T_0, T_1) = 0 \\
&\quad \frac{\partial^2}{\partial {T_0}^2} w_0 (T_0, T_1) + v_0 (T_0, T_1) = 0, \forall |w| < 1 \\
&\quad D_0 v_{0+} = D_0 v_{0-}, D_0 w_{0+} = -R D_0 w_{0-}, for\, |w| = 1
\end{aligned} \tag{11}$$

$$\begin{aligned}
&\epsilon^1 : \\
&\frac{\partial^2}{\partial {T_0}^2} v_1 (T_0, T_1) + v_1 (T_0, T_1) = -2 \frac{\partial^2}{\partial T_0 \partial T_1} v_0 (T_0, T_1) - \lambda \frac{\partial}{\partial T_0} v_0 (T_0, T_1) \\
&+ A \sin (\Omega T_0) - w_0 (T_0, T_1) + v_0 (T_0, T_1) \\
&\frac{\partial^2}{\partial {T_0}^2} w_1 (T_0, T_1) + v_1 (T_0, T_1) = -2 \frac{\partial^2}{\partial T_0 \partial T_1} w_0 (T_0, T_1) - \lambda \frac{\partial}{\partial T_0} v_0 (T_0, T_1) \\
&+ A \sin (\Omega T_0) - w_0 (T_0, T_1) + v_0 (T_0, T_1), \forall |w| < 1 \\
&v_{1+} = v_{1-}, w_{1+} = w_{1-} \\
&D_0 v_{1+} + D_1 v_{0+} = D_0 v_{1-} + D_1 v_{0-} \\
&D_0 w_{1+} + D_1 w_{0+} = -R(D_0 w_{1-} + D_1 w_{0-}), for\, |w| = 1
\end{aligned} \tag{12}$$

According to (11), the solution of $v_0$ and $w_0$ can be expressed in the following way:

$$v_0 (T_0, T_1) = A (T_1) \sin (T_0 + \theta (T_1)) \tag{13}$$

$$w_0 (T_0, T_1) = A (T_1) \sin (T_0 + \theta (T_1)) + B (T_1) T_0 + C (T_1) \tag{14}$$

The time dependance is omitted for simplification of notation. Solutions with two symmetrical impacts per period are studied herein. The conditions of periodicity are as follows:

$$w_0 (0) = 1, w_0 (\pi) = -w_0 (0), D_0 w_{0+} (\pi)) = -D_0 w_{0+} (0)) \tag{15}$$

After introduction of (13) and (14) into (15), it becomes:

$$B_1 = -2 \frac{C_1}{\pi}, \sin (\theta) = \frac{1 - C_1}{A}, \cos (\theta) = 2 \frac{\sigma C_1}{\pi A} \tag{16}$$

where $\sigma = (1 - R)/(1 + R)$, the second and third equation are combined,a relation between the slow variables A and C is obtained as follow:

$$A^2 = (1 - C)^2 + 4 \frac{C^2 \sigma^2}{\pi^2} \tag{17}$$

It represents the slow invariant manifold (SIM) of the system, its stability is showed in Fig.2:

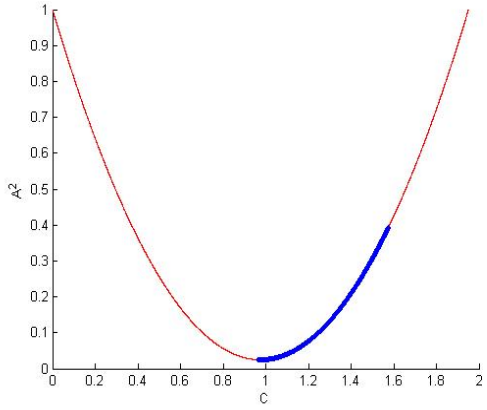


Figure 2: SIM of the problem for R=0.6, b=0.015. Stable (thick) and unstable (thin) branches.

In order to study the dynamics of the system under harmonic forcing, Eq. (12) is analyzed. To identify terms that produce secular terms, the equation of motion of the VI-NES is developed in Fourier series:

$$B\left(T_1\right)T_0 + C\left(T_1\right) = \boxed{F\left(T_1\right)\sin\left(T_0 + \zeta\left(T_1\right)\right)} + \boxed{NSF} \tag{18}$$

Eq. (18) has two components: the first one is that with the same frequency with LO and the second one are those that do not have the same frequency with the LO denoted by NSF and donot produce secular terms in the following analysis.

We are interested in the behavior of the system in the vicinity of the 1:1 resonance where LO oscillates with a frequency close to external forcing while the VI-NES operates with two symmetric impact per cycle. A detuning parameter($\delta$) representing the nearness of the excitation frequency $\Omega$ to the reduced natural frequency of the LO is introduced:

$$\Omega = 1 + \epsilon\,\delta \tag{19}$$

After substitution of (18) and (19) into (12) and eliminating terms that produce secular terms give:

$$\begin{aligned}
&\frac{\partial^2}{\partial {T_0}^2} v_1(T_0,T_1) + v_1(T_0,T_1) = -2\left(\frac{d}{dT_1}C(T_1)\right)\cos(T_0+\theta(T_1)) \\
&+ 2\,C(T_1)\sin(T_0+\theta(T_1))\,\frac{d}{dT_1}\theta(T_1) \\
&- \lambda\,C(T_1)\cos(T_0+\theta(T_1)) + A\sin(\Omega\,T_0) \\
&- F(T_1)\sin(T_0+\zeta(T_1)) + NFW
\end{aligned} \tag{20}$$

Substitution of (19) into (20) and then elimination of the secular terms:

$$\begin{aligned}
&-2\left(\frac{d}{dT_1}C(T_1)\right)\cos(\theta(T_1)) + 2\,C(T_1)\left(\frac{d}{dT_1}\theta(T_1)\right)\sin(\theta(T_1)) \\
&- \lambda\,C(T_1)\cos(\theta(T_1)) + A\sin(T_1\sigma) - F(T_1)\sin(\zeta(T_1)) = 0 \\
&2\left(\frac{d}{dT_1}C(T_1)\right)\sin(\theta(T_1)) + 2\,C(T_1)\left(\frac{d}{dT_1}\theta(T_1)\right)\cos(\theta(T_1)) \\
&+ \lambda\,C(T_1)\sin(\theta(T_1)) + A\cos(T_1\sigma) - F(T_1)\cos(\zeta(T_1)) = 0
\end{aligned} \tag{21}$$

After rearrangement, it becomes:

$$\begin{aligned}
&\frac{d}{dT_1}C(T_1) \\
&= -1/2\,\lambda\,C(T_1) + 1/2\,A\sin(-\theta(T_1)+T_1\sigma) \\
&- 1/2\,F(T_1)\sin(-\theta(T_1)+\zeta(T_1)) \\
&\frac{d}{dT_1}\theta(T_1) \\
&= 1/2\,\frac{-A\cos(-\theta(T_1)+T_1\sigma) + F(T_1)\cos(-\theta(T_1)+\zeta(T_1))}{C(T_1)}
\end{aligned} \tag{22}$$

Introducing $\gamma(T_1) = -\theta(T_1) + T_1\sigma$ and eliminating the derivative of $C$ and $\gamma$ to zero, the following relations between C and B are obtained, $K_1$ and $K_2$ are not expressed here because of there lengths.

$$A^2 = K_1 C, A^2 = K_2 C, \tag{23}$$

Then the fixed points of system can be obtained by solving Eq. (17) and Eq. (23).

# 3 VI-NES optimization

In this section, various response regimes with respect to the length of cavity are identified and then a criteria is defined for the optimization of the VI-NES, in which the energy pumping is the most efficient.

The parameters for simulation are as follows:

$$\begin{aligned} &m1 = 3.807kg, c1 = 2.53Ns/m, k1 = 11.68 * 103N/m, \\ &m2 = 0.032kg, b = 0.015m, R = 0.6, \epsilon = 0.84\%, \lambda = 1.43, \sigma = 0 \end{aligned} \tag{24}$$

$N^0$ is the number of simulation, $b$ and $b0$ are the value and reference value of length of cavity respectively. $G$ and $G0$ are corresponding nondimensional value and reference value of force respectively. Parameters decided by $b$ are showed in Tab.1.

| value | $b0 = 0.015m/G0 = 1.0131$ | | | | | | | |
|---|---|---|---|---|---|---|---|---|
| $N^0$ | 8 (a) | 3 (b) | 4 (c) | 1 (d) | 2 (e) | 5 (f) | 6 (g) | 7 (h) |
| $G/G0$ | 2.4 | 1.6 | 1.1 | 1 | 0.95 | 0.75 | 0.5 | 0.1 |
| $b/b0$ | 1/2.4 | 1/1.6 | 1/1.1 | 1/1 | 1/0.95 | 1/0.75 | 1/0.5 | 1/0.1 |

Table 1: Simulation parameters

Fig.3 demonstrates the variance of the amplitude of the LS with respect to length of cavity in Tab.1, which is obtained by FFT when the responses enter into a stable state by time simulation. It is seen that the amplitude of LO decreases at the first place until some point and then increases again with the decrease of the length of the cavity.

From the above simulations, the following six regimes can be expected in Fig.4 among which four regimes are observed and

case 1: as $b \to \infty$ ,VI-NES has no influence in LO.

case 2: with decrease of $b$, the response regime with less than two impacts per cycle of LO occurs, the typical time response is showed in Fig.5(a).

case 3: the regime 1:1 symmetric resonance occurs with further decrease of $b$, which can be analyzed through previous introdued procedure, the time typical response is showed in Fig.5(b).

case 4: further increase of $b$ cause exist the occurence of SMR, in which one part of response is in 1:1 resonance, and the other part is like case 2. It is correspondant to Fig.3 (e) and the typical time response is showed in Fig.5(c).

case 5: when the value of $b$ is decreased small enough, regime with more than two impacts per period of LO occurs and the typical time response is showed in Fig.5(d).

case 6: $b \to 0$, VI-NES will become one part of LO.

From Tab.1, Fig.3 and Fig4, we can conclude that the reponse regime of SMR (case 4) is the most efficient regime for energy pumping between LO and VI-NES, although which point during the SMR zone is the most efficient is not clear. Therefore, the idea of optimization is to find the most efficient zone.

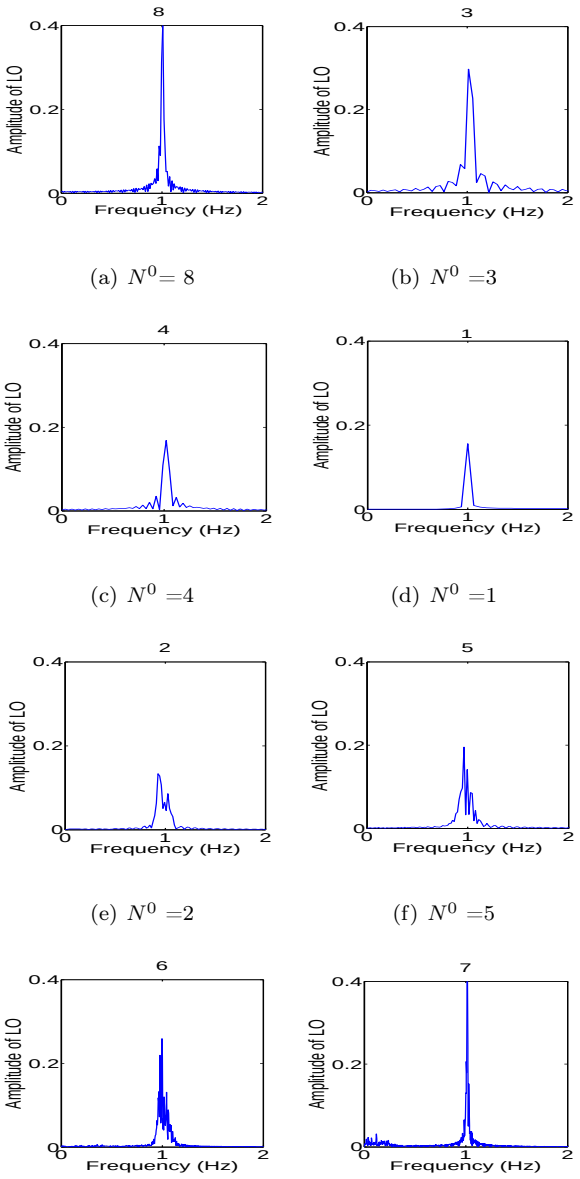


(a) $N^0$= 8 (b) $N^0$ =3

(c) $N^0$ =4 (d) $N^0$ =1

(e) $N^0$ =2 (f) $N^0$ =5

(g) $N^0$ =6 (h) $N^0$ =7

Figure 3: Influence of cavity's length to the LO's amplitude

# 4 VI-NES optimization

In this part, a detailed simulation about SMR is showed in the first place. Then the existence conditions of SMR are studied. A SMR ($b = b0/0.75$) with the

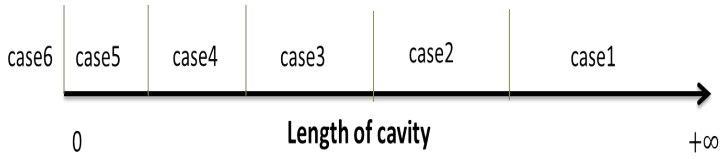


Figure 4: Response regime of LO with respect to the length of cavity

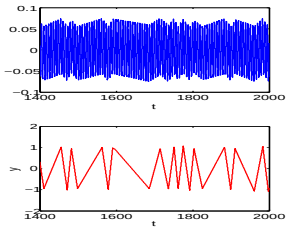

(a) case 2

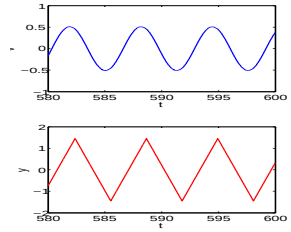

(b) case 3

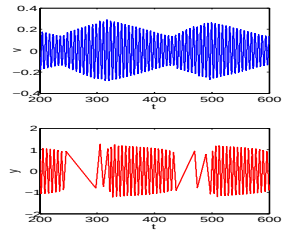

(c) case 4

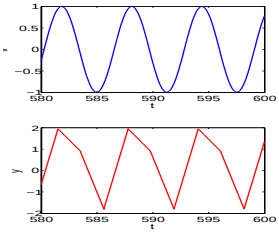

(d) case 5

Figure 5: Typical reponse regime of LO coupled with VI-NES

same parameters in the previous part of Fig.3 is studied here in detail, and initial conditions are selected around SIM. It is showed that there does not exist any stable or unstable points which is demonstrated in Fig. 6 (a) and the time simulation results is presented in Fig. 6 (b)(c).

When only the value of $G$ instead of $b$ is changed, there exist only two situations which can be represented by $\sigma = 0$ and $\sigma = -2$ as follows:

situation 1: $\sigma = 0$

The stable response of resonance 1:1 will disappear with the decrease of G and then the SMR will occur. The limit point in this situation is showed in the Fig. 7 (c), in which the stable point (red circle) reaches the lowest point of the curve.

Situation 2: $\sigma = -2$

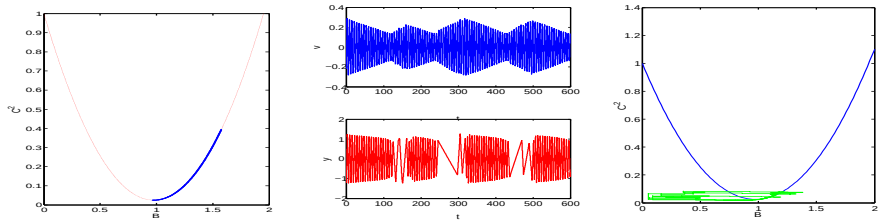

(a) Fixed points (b) Time reponse (c) Reponse trace between LO and VI-NES

Figure 6: Analysis for the case b=b0/0.75: (a) fixed points, (b) time response, (c) response trace between LO and VI-NES

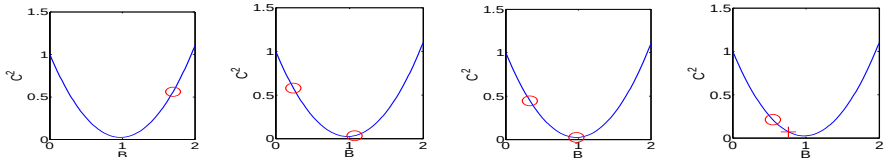

(a) (b) (c) (d)

Figure 7: The first case entering into SMR: stable (circle) and unstable (cross) fixed points.

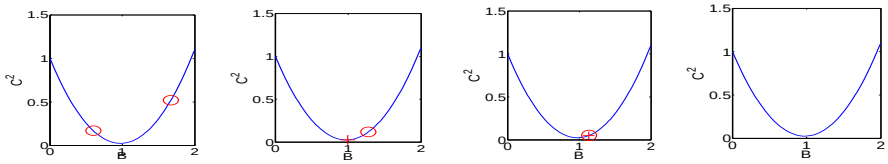

(a) (b) (c) (d)

Figure 8: The second case entering into SMR: stable (circle) and unstable (cross) fixed points.

In this situation, as the value of G decreases, the two points, one stable and one unstable, meet with each other in the left stable branch of the curve and then disappear together, as is demonstrated in Fig. 8 (c). Then there must be a critical value $\sigma$ between the two case, where these two situations encounter together.

Therefore, for any parameters of LO, there must exist a relationship between $\sigma$,$b$ and $G$ to trigger the occurrence of SMR which is calculated with the

theoretical results and is showed in Fig.9.

Some further simulations have been done around the curve, among which rose pentagram represents case5, rose circle represents case 2, red diamond represents case 4 and blue square represents case3.

According to the Fig.9, the optimization procedure can be done in the following way:

step1: measure of the parameters and the working conditions of LO like intervals of the amplitude and frequency of exciting force.

step2: calculate the optimization boundary curve as reference to design the paramters of VI-NES.

step3: for the known interval of $\sigma$, choose $G$ to get the SMR the most wide possible, then according to the relationship between G , F and b, design b the length of the cavity to let the G to meet the requirement in Fig.9.

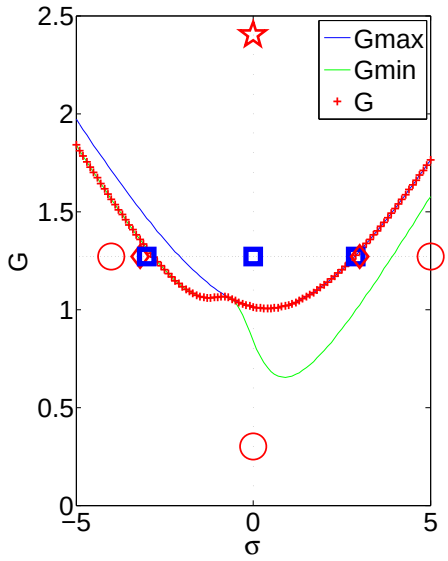


Figure 9: Boundary optimization for SMR with a VI-NES

## 5 Conclusion

The dynamic response of a two degrees of freedom system comprising a linear oscillator, subjected to an imposed harmonic displacement, with embedded vibro-impact nonlinear energy sink (VI-NES) is studied already theoretical and experimental. Therefore this paper is focused on the design optimization of

VI-NES for the most efficient energy pumping. Firstly, four typical response regimes have been observed with respect to the variance of the length of cavity and the SMR is proved to be the most efficient regime for vibration reduction. Secondly, two different limits between the regime 1:1 resonance and SMR can be obtained analytically, in which the SMR starts to exist. Based on this idea, a relationship between parameters and the occurrence of SMR is established, which is proved numerically. For future experiment and application, one optimization procedure for the design of VI-NES is presented.

## Reference

[1] O.V. Gendelman, L.I. Manevitch, A.F. Vakakis, and R. M'closkey. Energy pumping in nonlinear mechanical oscillators: Part i—dynamics of the underlying hamiltonian systems. *Journal of Applied Mechanics*, 68(1):34–41, 2001.

[2] A.F. Vakakis and O.V. Gendelman. Energy pumping in nonlinear mechanical oscillators: part ii—resonance capture. *Journal of Applied Mechanics*, 68(1):42–48, 2001.

[3] D.M. McFarland, L.A. Bergman, and A.F. Vakakis. Experimental study of non-linear energy pumping occurring at a single fast frequency. *International Journal of Non-Linear Mechanics*, 40(6):891–899, 2005.

[4] E. Gourdon, N.A. Alexander, C.A. Taylor, C.H. Lamarque, and S. Pernot. Nonlinear energy pumping under transient forcing with strongly nonlinear coupling: Theoretical and experimental results. *Journal of sound and vibration*, 300(3):522–551, 2007.

[5] G. Kerschen, J.J. Kowtko, D.M. McFarland, L.A. Bergman, and A.F. Vakakis. Theoretical and experimental study of multimodal targeted energy transfer in a system of coupled oscillators. *Nonlinear Dynamics*, 47(1-3):285–309, 2007.

[6] O.V. Gendelman. Bifurcations of nonlinear normal modes of linear oscillator with strongly nonlinear damped attachment. *Nonlinear Dynamics*, 37(2):115–128, 2004.

[7] Y. Starosvetsky and O.V. Gendelman. Strongly modulated response in forced 2dof oscillatory system with essential mass and potential asymmetry. *Physica D: Nonlinear Phenomena*, 237(13):1719–1733, 2008.

[8] E. Gourc, G. Michon, S. Seguy, and A. Berlioz. Experimental investigation and design optimization of targeted energy transfer under periodic forcing. *Journal of Vibration and Acoustics*, 136(2):021021, 2014.

[9] O.V. Gendelman and T. Bar. Bifurcations of self-excitation regimes in a van der pol oscillator with a nonlinear energy sink. *Physica D: Nonlinear Phenomena*, 239(3):220–229, 2010.

[10] Y.S. Lee, A.F. Vakakis, L.A. Bergman, D.M. McFarland, and G. Kerschen. Suppression aeroelastic instability using broadband passive targeted energy transfers, part 1: Theory. *AIAA journal*, 45(3):693–711, 2007.

[11] Y.S. Lee, G. Kerschen, D.M. McFarland, W.J. Hill, C. Nichkawde, T.W. Strganac, L.A. Bergman, and A.F. Vakakis. Suppressing aeroelastic instability using broadband passive targeted energy transfers, part 2: experiments. *AIAA journal*, 45(10):2391–2400, 2007.

[12] O.V. Gendelman, A.F. Vakakis, L.A. Bergman, and D. M. McFarland. Asymptotic analysis of passive nonlinear suppression of aeroelastic instabilities of a rigid wing in subsonic flow. *SIAM Journal on Applied Mathematics*, 70(5):1655–1677, 2010.

[13] B. Vaurigaud, L.I. Manevitch, and C.H. Lamarque. Passive control of aeroelastic instability in a long span bridge model prone to coupled flutter using targeted energy transfer. *Journal of Sound and Vibration*, 330(11):2580–2595, 2011.

[14] E. Gourc, S. Seguy, G. Michon, and A. Berlioz. Delayed dynamical sytem strongly coupled to a nonlinear energy sink: application to machining chatter. In *MATEC Web of Conferences*, volume 1, page 05002. EDP Sciences, 2012.

[15] O.V. Gendelman. Targeted energy transfer in systems with non-polynomial nonlinearity. *Journal of Sound and Vibration*, 315(3):732–745, 2008.

[16] C.H. Lamarque, O.V. Gendelman, A.T. Savadkoohi, and E. Etcheverria. Targeted energy transfer in mechanical systems by means of non-smooth nonlinear energy sink. *Acta mechanica*, 221(1-2):175–200, 2011.

[17] A.T. Savadkoohi, C.H. Lamarque, and Z. Dimitrijevic. Vibratory energy exchange between a linear and a nonsmooth system in the presence of the gravity. *Nonlinear Dynamics*, 70(2):1473–1483, 2012.

[18] F. Nucera, A.F. Vakakis, D.M. McFarland, L.A. Bergman, and G. Kerschen. Targeted energy transfers in vibro-impact oscillators for seismic mitigation. *Nonlinear Dynamics*, 50(3):651–677, 2007.

[19] F. Nucera, F. Lo Iacono, D.M. McFarland, L.A. Bergman, and A.F. Vakakis. Application of broadband nonlinear targeted energy transfers for seismic mitigation of a shear frame: Experimental results. *Journal of sound and vibration*, 313(1):57–76, 2008.

[20] Y.S. Lee, F. Nucera, A.F. Vakakis, D.M. McFarland, and L.A. Bergman. Periodic orbits, damped transitions and targeted energy transfers in oscillators with vibro-impact attachments. *Physica D: Nonlinear Phenomena*, 238(18):1868–1896, 2009.

[21] O.V. Gendelman. Analytic treatment of a system with a vibro-impact nonlinear energy sink. *Journal of Sound and Vibration*, 331(21):4599–4608, 2012.

[22] E. Gourc, G. Michon, S. Seguy, and A. Berlioz. Theoretical and experimental study of an harmonically forced vibro-impact nonlinear energy sink. *ASME Journal of Vibration and Acoustics (Accepted)*.